Synthesis of porous lignin xanthate resin for Pb^{2+} removal from aqueous solution

Zhili Li, Yan Kong, Yuanyuan Ge

PII: S1385-8947(15)00160-6
DOI: http://dx.doi.org/10.1016/j.cej.2015.01.123
Reference: CEJ 13240

To appear in: *Chemical Engineering Journal*

Received Date: 21 December 2014
Revised Date: 28 January 2015
Accepted Date: 29 January 2015

Please cite this article as: Z. Li, Y. Kong, Y. Ge, Synthesis of porous lignin xanthate resin for Pb^{2+} removal from aqueous solution, *Chemical Engineering Journal* (2015), doi: http://dx.doi.org/10.1016/j.cej.2015.01.123

Synthesis of porous lignin xanthate resin for Pb^{2+} removal from aqueous solution

Zhili Li[1, 2], Yan Kong[1], Yuanyuan Ge[*1]

[1]*School of Chemistry & Chemical Engineering, Guangxi Key Laboratory of Petrochemical Resource Processing and Process Intensification Technology, Guangxi University, Nanning, 530004, China*

[2]*School of Engineering and Applied Sciences, Harvard University, Cambridge, MA, 02138, USA*

Abstract

A new lignin xanthate resin (LXR) was synthesized by a two-step reaction from alkaline lignin and carbon disulfide. It was characterized by FT-IR, SEM and element analysis. An ordered porous structure is observed on LXR. Batch adsorption including equilibrium isotherms, kinetics, and the effects of pH, dosage and temperature on the adsorption of Pb^{2+} by LXR were systematically studied. LXR shows a 4.8 times higher adsorption capacity than alkaline lignin at 30 ℃ that is attributed to the incorporation of xanthate groups and porous structure. Thermodynamic parameters, involving ΔH^o, ΔS^o and ΔG^o were also calculated from graphical interpretation of the experimental data. Negative values of ΔG^o indicate the adsorption process of Pb^{2+} by LXR is spontaneous. The positive value of ΔH^o confirms the endothermic adsorption in nature. The high adsorption capacity of LXR, together with its feasible preparation, biocompatibility and environmentally friendliness, open new perspectives in the potential use for wastewater treatment.

[*] Corresponding author: School of Chemistry & Chemical Engineering, Guangxi University, Nanning, 530004, China. Email: geyy@gxu.edu.cn.

Keywords: Lignin; Xanthate; Adsorption; Heavy Metal; Wastewater

1. Introduction

Contamination by toxic metallic ions has been a major environmental problem with the development of industry [1, 2]. Lead is one of the most toxic metallic ions, which can accumulate in humans and cause serious damage to the hematopoietic system and cardiovascular system [3, 4]. The cleanup of toxic metallic ions from industrial effluent prior to discharge into the environment is necessary. Conventional methods for removing toxic metallic ions from wastewater include chemical precipitation, electrochemical treatment, adsorption, filtration, ion exchange and membrane separation [4-6]. Among them, adsorption is preferred due to its lower cost, high efficiency and various adsorbents being available [7]. Recently, great attention has been focused on the development of biomass adsorbents [8, 9].

Lignin, one of the main constituents of lignocellulose biomass, is the second abundant biopolymer on the earth [10]. Every year about 50 million tons of lignin is generated by the paper industries all over the world, but less than 10% is utilized [11]**.** Lignin contains phenol hydroxyl, alcoholic hydroxyl, carbonyl and carboxyl, methoxy, etc., which suggests it being potential in removal of metallic ions from wastewater as a low cost adsorbent [12]. However, lignin is a 3-dimensional, non-linear polymer, it is easy to form intermolecular hydrogen bonds that makes it unable to uncoil in water and wrap around large particles to form large stable flocks. As a result, the adsorption capacity of lignin for metallic ions is poor [13-16]. The weakness and handicaps

associated with existing lignin adsorbents necessitate the development of new types of lignin-based polymer by introduction of additional functional groups like amino, sulfonic and dithiocarbamate groups onto lignin matrix [10, 17, 18].

However, xanthate functionalized lignin has not been reported so far, which are expected to be an effective moiety for sorption of metallic ions from aqueous solution [19, 20]. Therefore, in this study, we synthesized a lignin xanthate resin (LXR) by a two-step method from alkaline lignin. Its structure was characterized by TF-IR, SEM and element analysis. The incorporation of xanthate functional groups onto lignin matrix may enhance its interaction with Pb^{2+} and an increase in adsorption capacity is expected. The influences of pH, dosage, temperature, contact time and initial concentration of Pb^{2+} on adsorption were studied. The adsorption kinetics and isotherms were fitted by pseudo-first-order, pseudo-second-order and Langmuir, Freundlich models, respectively. The adsorption thermodynamics were further analyzed by interpreting the experimental data.

2. Materials and methods

2.1. Materials

The chemicals including lead nitrate, carbon disulfide, formaldehyde, sodium hydroxide, hydrochloric acid, were purchased from Aladdin Chemicals, Beijing, China as analytical reagent grade. Alkaline lignin was obtained by precipitation from the black liquor (density=1.15 g/cm^3, pH=12.9, Nanpu Pulp Mill, China) with H_2SO_4 at a pH of 2.0.

2.2. Preparation of LXR

The LXR were prepared by a two-step method (as shown in Scheme1). *i*) Alkali lignin (10.0 g) and 100 mL distilled water was poured into a three-necked round-bottomed flask with an electric heating device, a motor stirrer, a thermometer, a dropping funnel, and a reflux condenser. The temperature was elevated to 80 ℃ and the pH was adjusted to 12.0 by NaOH. Formaldehyde (10.0 mL) was added drop-wisely into the flask for hydroxyl methylation reaction of 3h. After the reaction completed the mixture was cooled to 30℃. *ii*) Another part NaOH (4.0 g) was added into the flask, and carbon sulfide (10.0 mL) was added dropwisely. The reaction proceeded for 2 h at 30℃. After that, the mixture was precipitated at pH around 3.0 by 0.1M HCl and filtrated. The residue was washed with distilled water to neutral. Finally, a brown powder (i.e. LXR) was obtained after drying under vacuum (65 ℃) overnight and grinded.

2.3. Characterizations

Fourier transform infrared (FT-IR) spectroscopy of the samples was recorded on a FT-IR spectrophotometer (Thermo Nicolet 510, United States) using a KBr disk method and scanned in the range of 4000-400 cm^{-1}. SEM images were taken in a Hitachi SU8020 microscope by immobilizing the sample with conductive glue. Element analysis (EA) of dry samples was performed on a PE 2400 II (Perkin–Elmer, USA). Four elements, i.e., carbon, hydrogen, nitrogen and sulfur were determined.

2.4. Batch adsorption

The batch adsorption was carried out by mixing adsorbent with 50 mL Pb^{2+} aqueous solution. The mixture was agitated at 100 rpm in a thermostatic shaking incubator to reach the equilibrium. The effect of pH on the adsorption was studied in the range of 1.0-7.0 that was adjusted with dilute HCl or NaOH solution at 30 ℃. The effect of dosage on the adsorption was determined with different LXR dosage of 0.01-0.1 g/50 mL Pb^{2+} solution at 25 mg/L. Adsorption isotherms were studied at different initial Pb2+ concentration (10-100 mg/L) with a LXR dosage of 0.04 g/50 mL under temperature of 30, 40 and 50 ℃, respectively. Adsorption kinetics were carried out at 30 ℃ and pH 5.0 with different initial Pb^{2+} concentration (20, 50 and 100 mg/L). The samples were collected at predetermined time intervals and filtered immediately. The concentration of Pb^{2+} was determined by an inductively coupled plasma optical emission spectrometry (ICP-OES, optima 5300DV, PerkinElmer), with a Plasma gas flow 15 L/min and nebulizer gas flow of 0.6 L/min. The pump rate was 100 rpm and the sample uptake rate was 1.2 mL/min for 30s. The pipeline was washed by de-ionized water for 15 s at the intervals of each sampling. The wavelength was 220.4 nm. The adsorption capacity (q_e) was calculated by Eq. (1):

$$q_e\,(mg/\mathrm{g}) = \frac{V\,(C_0 - C_e)}{m} \tag{1}$$

where C_0 (mg/L) and C_e (mg/L) are the initial and final Pb^{2+} concentration. V (L) is the volume of the solution, and m (g) is the mass of LXR.

3. Results and discussion

3.1. Characterization of LXR

Fig. 1 shows the SEM images of the samples. As can be seen, the alkaline lignin (a) exhibits as amorphous plates/particles with some agglomeration. Inspiring, the LXR (b) exhibits an ordered porous structure with pore diameter below 100 nm that might be due to the crosslinking between lignin and formaldehyde molecules [21]. The morphology images demonstrate the amorphous lignin plates have been converted to porous compound after modification, which will increase the number of active sites in the surface of LXR and will be benefit for the adsorption of lead ions from aqueous solution.

The FT-IR spectra of lignin and LXR are shown in Fig. 2. The broad and intensive peaks around 3420 cm^{-1} can be assigned to hydroxyl group stretching. The peaks at 2925 cm^{-1} can be attributed to the symmetric and asymmetric C-H tensile vibration of methylene. The bands at 1600 cm^{-1}, contributed to aromatic skeletal vibration, and the bands at 837 cm^{-1}, attributed to C-H in-plane deformations in aromatic rings are also found in both LXR and lignin that suggests the aromatic nature of the samples [18]. The peaks at 1460 and 1380 cm^{-1} are assigned to -CH_2 symmetric scissoring and OH bending vibrations, respectively. The bands at 1130 cm^{-1} are due to the C-O antisymmetric bridge stretching. The bands around 1040 cm^{-1} are due to -CH_2-O- stretching vibration [22]. The appearance of new bands of LXR at 1220, 683 cm^{-1} should be attributed to C=S and C-S stretching, respectively [10].

The elemental analysis of dry samples show that LXR contains 46.16% C, 4.13%

H, 0.09% N and 6.65% S, respectively. The content of C of LXR decreases by comparing with alkaline lignin (C: 53.21%, H: 5.02%, N: 0.11%, S: 0.44%), while the contents of S distinctly increase to 6.65% after reacting with CS_2. These above analysis results prove that LXR had been successfully synthesized.

3.2. Batch adsorption

3.2.1 Effect of pH

The solution pH plays a critical important role in the adsorption of metal ions by various adsorbents [23]. It determines the level of electrostatic or molecular interaction between the adsorbent surface and the adsorbate owing to charge distribution on the material. In order to optimize the pH for maximum removal efficiency, adsorption experiment was conducted in the initial pH range from 1 to 7 at an initial Pb^{2+} concentration of 100 mg/L with a LXR dosage of 0.04 g/50mL. The results are shown in Fig. 3. It is seen that the removal efficiency is strongly dependent on the solution pH. The adsorption capacity of Pb^{2+} increases steadily to 62.5 mg/g with increasing pH from 1 to 5. The low uptake of Pb^{2+} at lower pH is attributed to the competitive adsorption of H^+ and Pb^{2+} on the LXR surface active sites [24, 25]. At higher pH value, the -CSSH groups will be ionized to negative $-CSS^-$ groups, and accordingly chelate with Pb^{2+}. Therefore a gradual increase of Pb^{2+} ions removal can be achieved with increasing pH. On the other hand, as pH > 6, the OH^- concentration increases and insoluble $Pb(OH)_2$ can be formed that will be contributes to the removal of Pb^{2+} [10]. In order to avoid the hydroxides precipitation interference, all the

following experiments were conducted at pH 5.0.

3.2.2. Effect of dosage

The adsorption of Pb^{2+} as a function of LXR dosage (pH=5.0, t=300 min, C_0=25 mg/L, T=30 ℃) was conducted and the results are shown in Fig. 4. As can be seen, the adsorption efficiency increases sharply from 35.1% to 93.5% as the LXR dosage increases from 0.01 to 0.04 g/50 mL, which can be assigned to the increasing surface area and number of active sites as the LXR dosage increases. When the LXR dosage increases from 0.04 to 0.1 g/50 mL, the adsorption efficiency for Pb^{2+} only increases 4.6%. Therefore, the practical LXR dosage for the removal of Pb^{2+} should be 0.04 g/50 mL.

3.2.3. Adsorption kinetics

The effect of contact time on adsorption capacity of LXR for Pb^{2+} was investigated (C_0=20, 50, 100 mg/L; pH=5.0; T=30 ℃, LXR dosage=0.04 g/50 mL) and the results are presented in Fig 5. It can be seen that the adsorption of Pb^{2+} on LXR can attain equilibrium around 90 min. The fast adsorption reflects good accessibility of LXR to lead ions that can be attributed to the availability of large number of vacant surface active sites, such as xanthate groups (base) for the sorption of lead ions (acid) [26]. Afterward the filling of vacant sites becomes difficult due to repulsive forces between lead ions adsorbed on LXR surface and lead ions from the bulk solution.

In order to interpret the differences in the adsorption kinetic rates and to examine the adsorption kinetic models. The adsorption kinetics were fitted by

pseudo-first-order and pseudo-second-order model [10, 27]:

$$\log(q_e - q_t) = \log q_e - \frac{k_1 t}{2.303} \quad (2)$$

$$\frac{t}{q_t} = \frac{1}{k_2 q_e^{\,2}} + \frac{t}{q_e} \quad (3)$$

where q_t is the amount adsorbed at time t (min), and q_e denotes the amount adsorbed at equilibrium, both in mg/g, k_1 (min^{-1}) and k_2 (g/mg min) represent the adsorption rate constants. The fitting results are presented in Fig 4 and Table 1.

It can be found from Table 1, the calculated correlation coefficient values (R^2) for first-order (0.9853-0.9957) and second-order (0.9615-0.9927) kinetics are found to be greater than 0.96, which shows the applicability of both these kinetic models. Thus in the present study, both the pseudo-first-order and pseudo-second-order kinetic expressions can be used in predicting the amount of Pb^{2+} adsorbed by LXR for the entire contact time. As seen in Table 1, the predicted q_e values (24.9, 56.1 and 63.4 mg/g, respectively) at different Pb^{2+} concentrations by pseudo first-order model are in good accordance with the experimental values (23.6, 53.9 and 62.6 mg/g, respectively). However, the predicted q_e values (32.1, 71.9 and 80.3 mg/g) by pseudo second-order are not closed to the experimental values. That indicates for the entire sorption period, pseudo first-order expression better predicts the sorption kinetics than the pseudo second-order model, which suggests the adsorption process depends on both the solution concentration and the number of available adsorption sites and the process is reversible with an equilibrium being established between the liquid and solid phases [28].

3.2.4. Adsorption isotherm

The adsorption isotherms of Pb^{2+} by LXR (pH=5.0; *T*=30, 40, 50 ℃) are displayed in Fig. 6 with alkaline lignin (pH=5.0; *T*=30 ℃) as a reference. As can be seen, the higher is the Pb^{2+} concentration, the more is the Pb^{2+} adsorption. The sharp increase in adsorption capacity is observed at low concentration that is due to excess active sites on LXR and the strong chelating force between xanthate groups and Pb^{2+} for mass transfer. At 30 ℃, the maximum adsorption capacity of Pb^{2+} by LXR is 62.6 mg/g which is a 4.8 fold higher than alkaline lignin (q_e=12.8 mg/g). According to the theory of hard and soft acid and base, soft bases are likely to form stable complexes with metals such as copper, cadmium and lead. Since xanthate group can be classified as soft base, the LXR shows a high tendency towards the acid Pb^{2+} rather than the alkaline lignin. It is also observed that the adsorption capacity of LXR for Pb^{2+} increases from 62.6 to 69.5 mg/g with an increase in temperature from 30 to 50 ℃, which indicates the endothermic nature of the adsorption process. This is because of the increase in temperature not only increases the diffusion rate of Pb^{2+} from the bulk solution to the adsorbent surface but also benefits the complexation between functional groups (i.e. $-OCSS^-$) and Pb^{2+}.

The equilibrium isotherms were analyzed in the light of two well-known models, Langmuir and Freundlich models. The Freundlich isotherm assumes of non-ideal sorption on heterogeneous surfaces, whereas Langmuir isotherm is used for the monolayer adsorption on a homogenous surface. Langmuir and Freundlich models can be presented by the following equations [29]:

$$q_e = \frac{q_{\max} b C_e}{1 + b C_e} \tag{4}$$

$$q_e = K_F C_e^{1/n} \tag{5}$$

where q_e (mg/g) is the amount of adsorbed Pb^{2+} per unit weight of adsorbent, and C_e (mg/L) is the Pb^{2+} concentration at equilibrium. q_{max} is the maximum amount of adsorption (mg/g), *b is* the adsorption constant (L/mg), K_F (mg/g) and *n* are Freundlich constants related to adsorption capacity and adsorption intensity. The value of *n* falling in the range of 1-10 indicates favorable adsorption.

The fitting of equilibrium data at different temperature by Freundlich and Langmuir equations was conducted and the results are presented in Fig 6 and Table 2. From Fig. 6 it is observed that the equilibrium data are very well represented by Langmuir equation. It is also observed from Table 2, the adsorption equilibrium data fit Freundlich and Langmuir equations with correlation coefficient values of R^2<0.78 and R^2>0.95, respectively. The maximum adsorption capacity of Pb^{2+} by LXR according to Langmuir model is 63.9, 66.3 and 71.1 mg/g, respectively, which is highly in agreement with the experimental value (62.6, 64.9 and 69.5 mg/g at 30, 40 and 50℃, respectively). The results are comparable with the adsorption capacities of the other biomass sorbents reported in literature [18, 30, 31]. The better fit of equilibrium data by Langmuir isotherm equation confirms the monolayer coverage of Pb^{2+} onto the homogenous surface of LXR which can be seen from the SEM image. As to Freundlich model, the calculated values of *n* which are found to be in the range of 1-10 indicating the adsorption being favorable.

3.2.5 Adsorption thermodynamics

Thermodynamic considerations of an adsorption process are necessary to conclude whether the process is spontaneous or not. The amounts of Pb^{2+} adsorbed at different temperatures 30, 40 and 50 ℃, at equilibrium have been used to obtain thermodynamic parameters for the adsorption process. The standard Gibbs free energy change (ΔG^o), standard enthalpy change (ΔH^o) and standard entropy change (ΔS^o) were determined by using Eqs. (6), (7) [32]:

$$\Delta G^o = -RT \ln k_d \tag{6}$$

$$\ln k_d = -\frac{\Delta H^o}{RT} + \frac{\Delta S^o}{R} \tag{7}$$

where k_d is the distribution coefficient, R is the gas constant (J/mol K). The effect of temperature on the adsorption of Pb^{2+} onto LXR is given from the plots and curves of the distribution coefficient values k_d versus temperatures in Fig. 7. It can be found that k_d increased with increasing temperature, a certification of endothermic adsorption in nature [25]. According to Eq. (7), the values of ΔH^o and ΔS^o can be calculated respectively from the slope and intercept of $\ln k_d$ versus $1/T$ plots. The calculated values of thermodynamic parameters are presented in Table 3.

From Table 3, the overall free energy changes during the adsorption process at 30, 40 and 50 ℃ are negative, corresponding to a spontaneous adsorption process of Pb^{2+} by LXR. The increase in absolute value of ΔG^o as temperature rising indicates that the adsorption process becomes more favorable at higher temperature. The positive value of +11.93 kJ/mol of the enthalpy change indicates that the adsorption is endothermic in nature. The positive value of entropy change (ΔS^o=56.49 J/K mol) suggests the randomness at the solid-solution interface increases during the adsorption of Pb^{2+} on

LXR [33].

4. Conclusion

Lignin xanthate resin (LXR) was prepared by a two-step method from alkaline lignin, which is easy for large scale production. The LXR contained an ordered porous structure with pore diameter below 100 nm. It was used as a new adsorbent for the removal of Pb^{2+} from aqueous solution. The adsorption kinetics is found to follow pseudo-first order model and the equilibrium data follows Langmuir isotherm model. The maximum adsorption capacity of LXR for Pb^{2+} is 64.9 mg/g at 30 ℃ according to Langmuir model. Higher adsorption capacity of LXR for Pb^{2+} rather than alkaline lignin is attributed to introduction of xanthate moiety and porous structure. The adsorption thermodynamics indicates that the adsorption process of Pb^{2+} on LXR is spontaneous and endothermic. The low cost, easy preparation and its efficient removal of Pb^{2+} from wastewater makes LXR being a great potent for the treatment of wastewater containing metallic ions.

Acknowledgments

We greatly acknowledge the support from the National Natural Science Foundation of China (21264002, 21464002), Guangxi Key Laboratory of Petrochemical Resource Processing and Process Intensification Technology (2013Z008, 2014Z002) and the Haina Project of Guangxi University and Training Program for Outstanding Young Teacher of Guangxi Higher Education Institutions.

References

[1] J. Choi, A. Ide, Y.B. Truong, I.L. Kyratzis, R.A. Caruso, High surface area mesoporous titanium-zirconium oxide nanofibrous web: a heavy metal ion adsorbent, J. Mater. Chem. A. 1 (2013) 5847-5853.

[2] N. Bolan, A. Kunhikrishnan, R. Thangarajan, J. Kumpiene, J. Park, T. Makino, M.B. Kirkham, K. Scheckel, Remediation of heavy metal(loid)s contaminated soils - To mobilize or to immobilize? J. Hazard. Mater. 266 (2014) 141-166.

[3] D. Chauhan, N. Sankararamakrishnan, Highly enhanced adsorption for decontamination of lead ions from battery wastewaters using chitosan functionalized with xanthate, Bioresource. Technol. 99 (2008) 9021-9024.

[4] T. Torres-Blancas, G. Roa-Morales, C. Fall, C. Barrera-Díaz, F. Ureña-Nuñez, T.B. Pavón Silva, Improving lead sorption through chemical modification of de-oiled allspice husk by xanthate, Fuel. 110 (2013) 4-11.

[5] A. Sotto, J. Kim, J.M. Arsuaga, G. Del Rosario, A. Martinez, D. Nam, P. Luis, B. Van der Bruggen, Binary metal oxides for composite ultrafiltration membranes, J. Mater. Chem. A. 2 (2014) 7054-7064.

[6] D.S. Tavares, A.L. Daniel-da-Silva, C.B. Lopes, N.J.O. Silva, V.S. Amaral, J. Rocha, E. Pereira, T. Trindade, Efficient sorbents based on magnetite coated with siliceous hybrid shells for removal of mercury ions, J. Mater. Chem. A. 1 (2013) 8134-8143.

[7] A. Abdolali, W.S. Guo, H.H. Ngo, S.S. Chen, N.C. Nguyen, K.L. Tung, Typical lignocellulosic wastes and by-products for biosorption process in water and wastewater treatment: A critical review, Bioresource. Technol. 160 (2014) 57-66.

[8] J. Roosen, K. Binnemans, Adsorption and chromatographic separation of rare earths with EDTA- and DTPA-functionalized chitosan biopolymers, J. Mater. Chem. A. 2 (2014) 1530-1540.

[9] A.C.S. Alcantara, M. Darder, P. Aranda, S. Tateyama, M.K. Okajima, T. Kaneko, M. Ogawa, E. Ruiz-Hitzky, Clay-bionanocomposites with sacran megamolecules for the selective uptake of neodymium, J. Mater. Chem. A. 2 (2014) 1391-1399.

[10] Y. Ge, D. Xiao, Z. Li, X. Cui, Dithiocarbamate functionalized lignin for efficient removal of metallic ions and the usage of the metal-loaded bio-sorbents as potential free radical scavengers, J. Mater. Chem. A. 2 (2014) 2136-2145.

[11] Z. Li, Y. Ge, Antioxidant activities of lignin extracted from sugarcane bagasse via different chemical procedures, Int. J. Biol. Macromol. 51 (2012) 1116-1120.

[12] A.B. Albadarin, A.H. Al-Muhtaseb, G.M. Walker, S.J. Allen, M.N.M. Ahmad, Retention of toxic chromium from aqueous phase by H3PO4-activated lignin: Effect of salts and desorption studies, Desalination. 274 (2011) 64-73.

[13] A. Kriaa, N. Hamdi, E. Srasra, Removal of Cu (II) from water pollutant with Tunisian activated lignin prepared by phosphoric acid activation, Desalination. 250 (2010) 179-187.

[14] D. Mohan, C.U. Pittman, P.H. Steele, Single, binary and multi-component adsorption of copper and cadmium from aqueous solutions on Kraft lignin—a biosorbent, J. Colloid. Interf. Sci. 297 (2006) 489-504.

[15] W.S. Peternele, A.A. Winkler-Hechenleitner, E.A. Gómez Pineda, Adsorption of Cd(II) and Pb(II) onto functionalized formic lignin from sugar cane bagasse, Bioresource. Technol. 68 (1999) 95-100.

[16] D. Parajuli, K. Inoue, K. Ohto, T. Oshima, A. Murota, M. Funaoka, K. Makino, Adsorption of heavy metals on crosslinked lignocatechol: a modified lignin gel, React. Funct. Polym. 62 (2005) 129-139.

[17] S. Laurichesse, L. Avérous, Chemical modification of lignins: Towards biobased polymers, Prog. Polym. Sci. 39 (2014) 1266-1290.

[18] Y. Ge, Z. Li, Y. Kong, Q. Song, K. Wang, Heavy metal ions retention by bi-functionalized lignin: Synthesis, applications, and adsorption mechanisms, J. Ind. Eng. Chem. 6 (2014) 4429-4436.

[19] S. Chakraborty, V. Tare, Role of various parameters in synthesis of insoluble agrobased xanthates for removal of copper from wastewater, Bioresource. Technol. 97 (2006) 2407-2413.

[20] M.H. Beyki, M. Bayat, S. Miri, F. Shemirani, H. Alijani, Synthesis, Characterization, and Silver Adsorption Property of Magnetic Cellulose Xanthate from Acidic Solution: Prepared by One Step and Biogenic Approach, Ind. Eng. Chem. Res. 53 (2014) 14904-14912.

[21] Z. Li, Y. Ge, Extraction of Lignin from Sugar Cane Bagasse and its Modification into a High Performance Dispersant for Pesticide Formulations, J. Brazil. Chem. Soc. 22 (2011) 1866-1871.

[22] S. Laurichesse, L. Avérous, Chemical modification of lignins: Towards biobased polymers, Prog. Polym. Sci. 39 (2014) 1266-1290.

[23] M.J.C. Calagui, D.B. Senoro, C. Kan, J.W.L. Salvacion, C.M. Futalan, M. Wan, Adsorption of indium(III) ions from aqueous solution using chitosan-coated bentonite beads, J. Hazard. Mater. 277 (2014) 120-126.

[24] M.L.P. Dalida, A.F.V. Mariano, C.M. Futalan, C. Kan, W. Tsai, M. Wan, Adsorptive removal of Cu(II) from aqueous solutions using non-crosslinked and crosslinked chitosan-coated bentonite beads, Desalination. 275 (2011) 154-159.

[25] B. Kannamba, K.L. Reddy, B.V. AppaRao, Removal of Cu(II) from aqueous solutions using chemically modified chitosan, J. Hazard. Mater. 175 (2010) 939-948.

[26] Y. Ge, Q. Song, Z. Li, A Mannich base biosorbent derived from alkaline lignin for lead removal from aqueous solution, J. Ind. Eng. Chem. In press.

[27] S. Malamis, E. Katsou, A review on zinc and nickel adsorption on natural and modified zeolite, bentonite and vermiculite: Examination of process parameters, kinetics and isotherms, J. Hazard. Mater. 252-253 (2013) 428-461.

[28] S. Sen Gupta, K.G. Bhattacharyya, Kinetics of adsorption of metal ions on inorganic materials: A review, Adv. Colloid. Interface. 162 (2011) 39-58.

[29] M.D. Meitei, M.N.V. Prasad, Adsorption of Cu (II), Mn (II) and Zn (II) by Spirodela polyrhiza (L.) Schleiden: Equilibrium, kinetic and thermodynamic studies, Ecol. Eng. 71 (2014) 308-317.

[30] M. Ghasemi, M. Naushad, N. Ghasemi, Y. Khosravi-fard, Adsorption of Pb(II) from aqueous solution using new adsorbents prepared from agricultural waste: Adsorption isotherm and kinetic studies , J. Ind. Eng. Chem. 20 (2014) 2193-2199.

[31] P.S. Keng, S.L. Lee, S.T. Ha, Y.T. Hung, S.T. Ong, Removal of hazardous heavy metals from aqueous environment by low-cost adsorption materials, Environ. Chem. Lett. 12 (2014) 15-25.

[32] Y. Liu, Is the Free Energy Change of Adsorption Correctly Calculated? J. Chem. Eng. Data. 54 (2009) 1981-1985.

[33] Ö. Gök, A. Özcan, B. Erdem, A.S. Özcan, Prediction of the kinetics, equilibrium and thermodynamic parameters of adsorption of copper(II) ions onto 8-hydroxy quinoline immobilized bentonite, Colloid. Surface. A. 317 (2008) 174-185.

Figure captions

Scheme 1. The synthetic diagram of LXR.

Fig. 1. SEM images of (a) lignin and (b) LXR

Fig. 2. FT-IR spectra of lignin (a), LXR (b).

Fig. 3. Effect of pH on adsorption capacity of Pb^{2+} by LXR.

Fig. 4. Effect of LXR dosage on the adsorption efficiency of Pb^{2+} by LXR.

Fig. 5. Adsorption kinetics and the fitting results by pseudo first-order and pseudo second-order models.

Fig. 6. Adsorption isotherms and the fitting results by Langmuir and Freundlich models.

Fig. 7. Plot of $\ln k_d$ against $1/T$ for the adsorption of Pb^{2+} on LXR.

Table 1. Kinetic parameters for the adsorption of Pb^{2+} by LXR.

C_0 (mg/L)	Experimental (mg/g)	Pseudo-first-order			Pseudo-second-order		
		$k_1 \times 10^{-2}$	q_e	R^2	$k_2 \times 10^{-4}$	q_e	R^2
20	23.6	2.25	24.9	0.9853	6.53	32.1	0.9615
50	53.9	2.26	56.1	0.9926	2.97	71.9	0.9746
100	62.6	2.27	63.4	0.9957	2.78	80.3	0.9927

Table 2. Fitting results of adsorption isotherms by Langmuir and Freundlich models.

T (℃)	Experimental (mg/g)	Langmuir model			Freundlich model		
		q_{max}	B	R_2	K_F	n	R_2
30	62.6	63.9	0.677	0.9561	29.9	4.83	0.7695
40	64.9	66.3	0.809	0.9619	32.5	5.04	0.7758
50	69.5	71.1	0.907	0.9507	35.4	5.05	0.7550

Table 3. Thermodynamic parameters for the adsorption of Pb^{2+} on LXR.

ΔG^o (kJ/mol)			ΔH^o (kJ/mol)	ΔS^o (J/K mol)
30 ℃	40 ℃	50 ℃		
			11.93	56.49
-5.17	-5.81	-6.29		

Scheme 1.

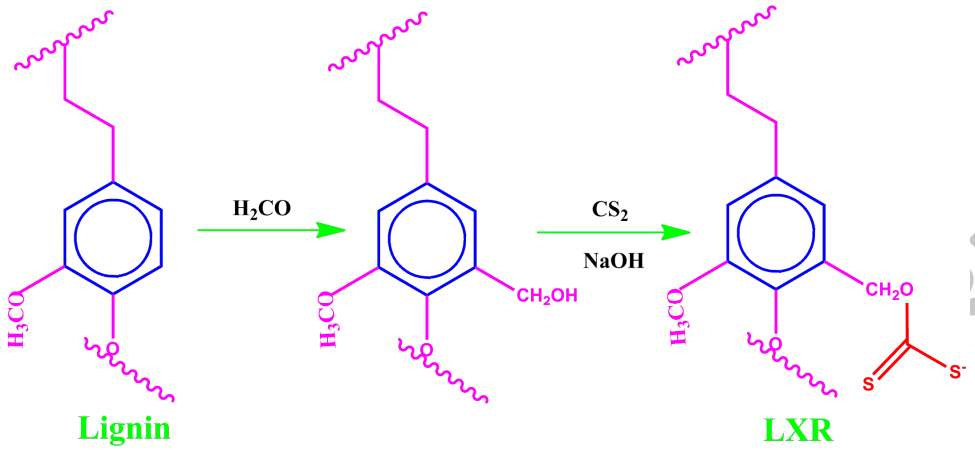

Fig. 1.

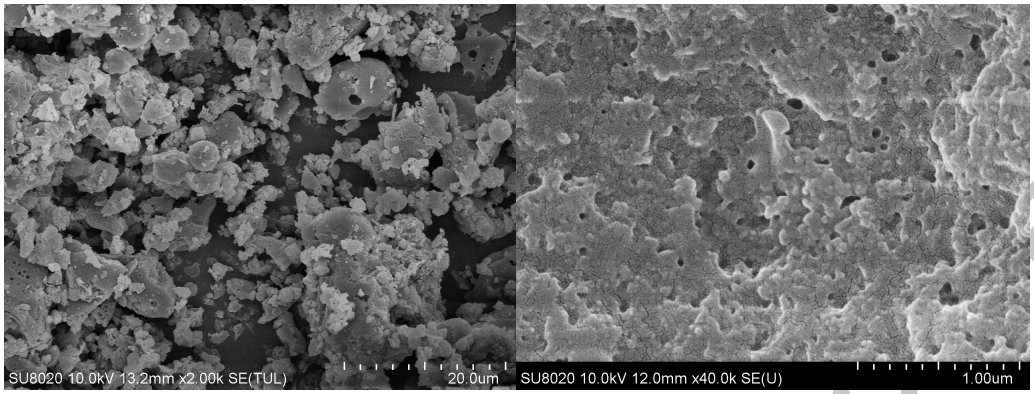

(a) **(b)**

Fig. 2.

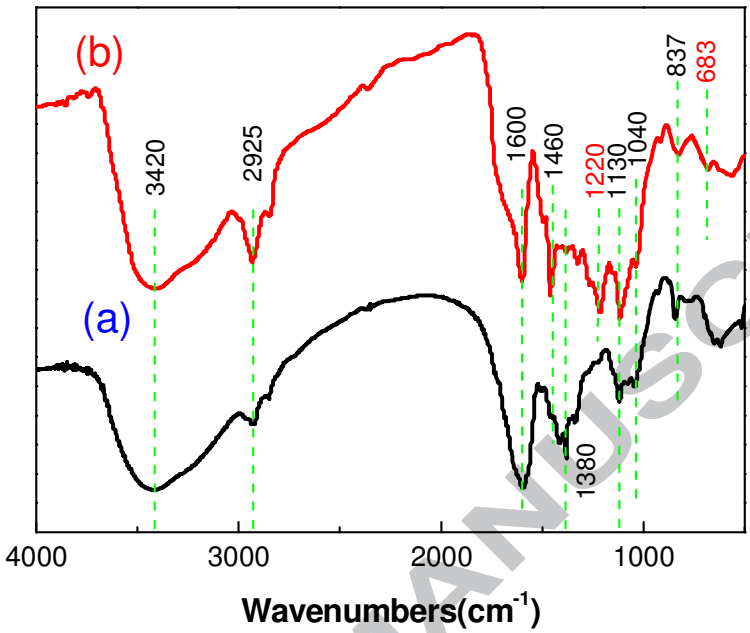

Fig. 3.

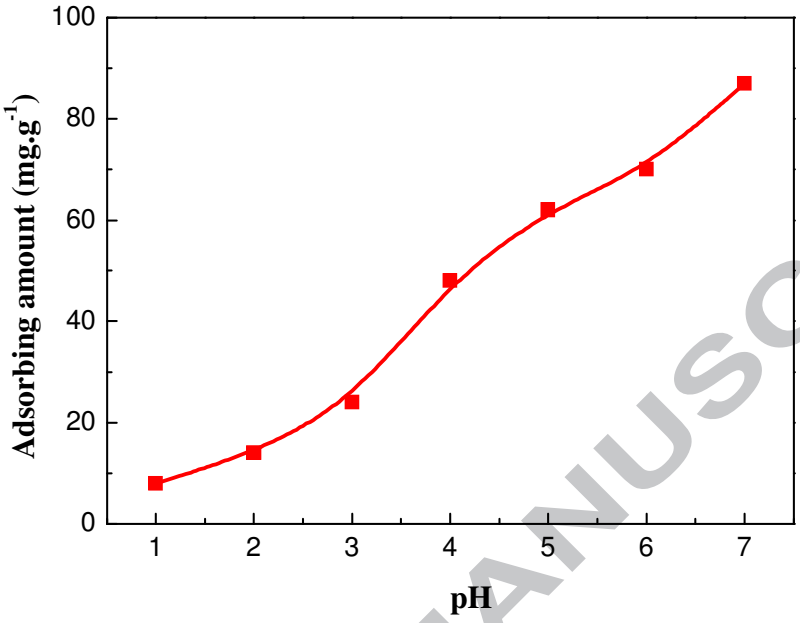

Fig. 4.

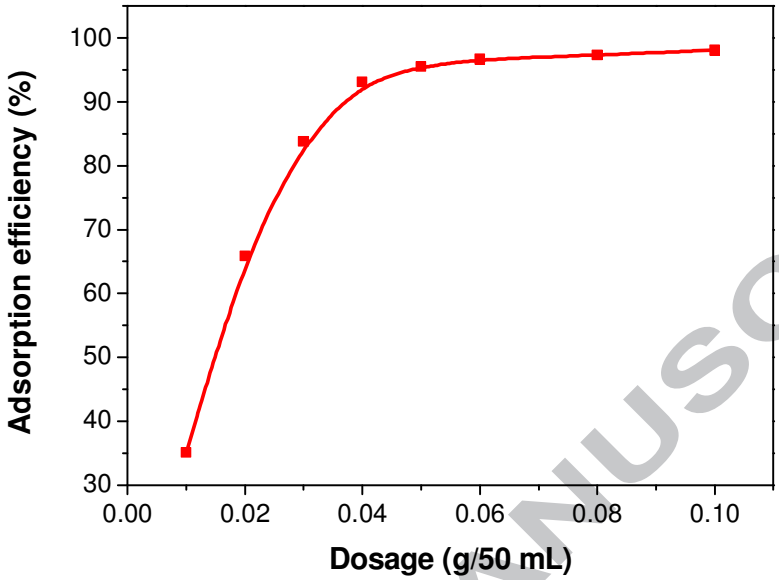

Fig. 5.

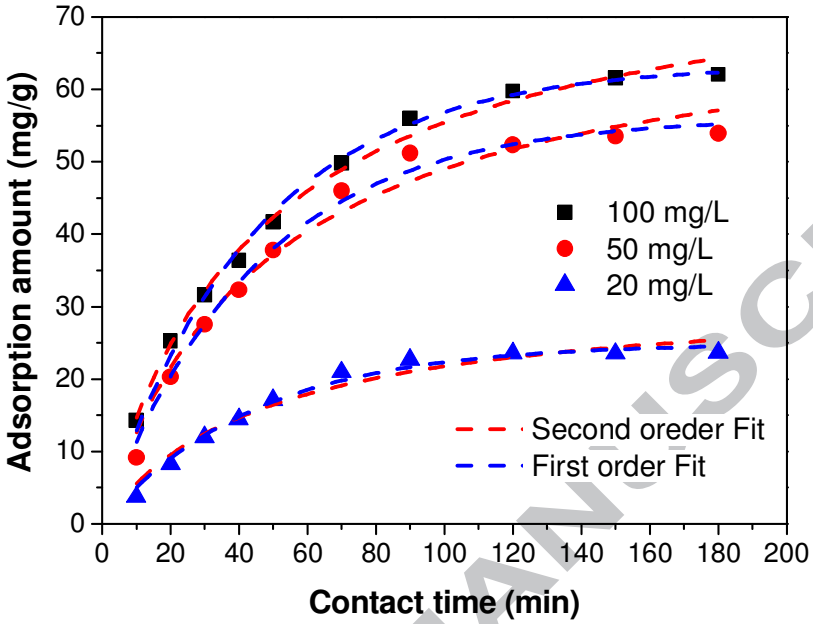

Fig. 6.

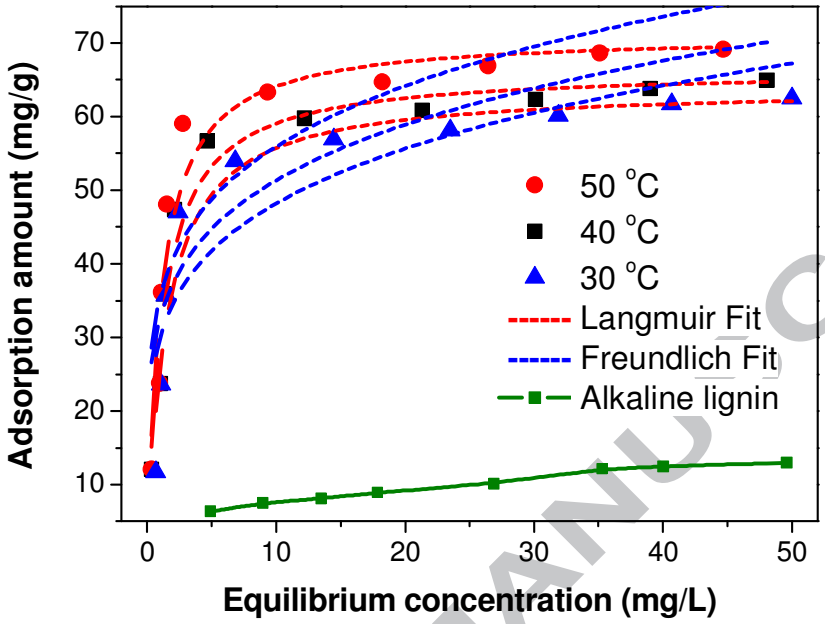

Fig. 7.

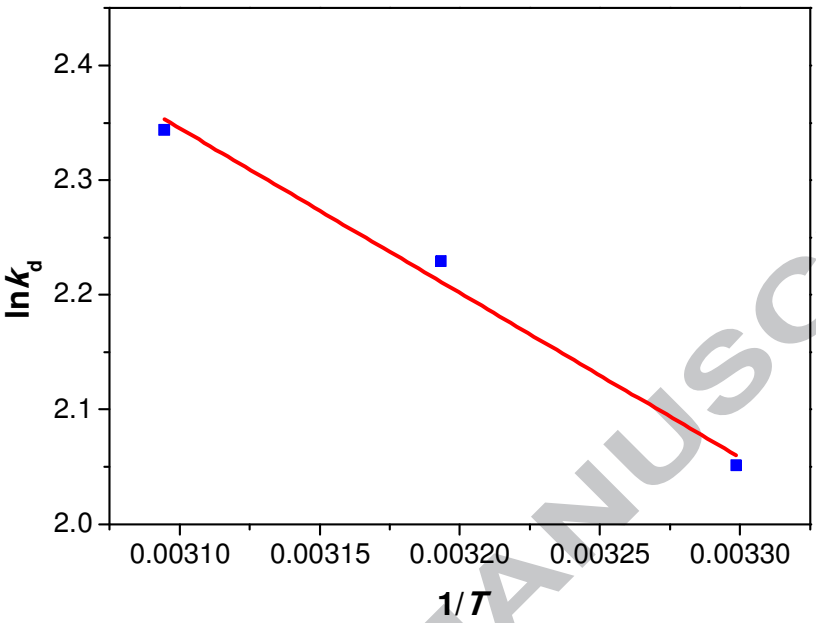

Highlights

- A lignin xanthate resin (LXR) was newly synthesized by a two-step method
- This method is easy for large-scale production
- The LXR contains an order porous structure (d_p<100 nm)
- The LXR showed a 4.8 times higher adsorption capacity than alkaline lignin
- The adsorption of Pb^{2+} by LXR is spontaneous and endothermic